The tectonic stress field evolution of India since the Oligocene

R. D. Müller[1,*], V. Yatheesh[2], M. Shuhail[2]

[1]EarthByte Group, School of Geosciences, University of Sydney, NSW 2006, Australia

[2]CSIR-National Institute of Oceanography, Dona Paula, Goa - 403 004, India

Gondwana Research, in revision

* Corresponding author

E-mail: dietmar.muller@sydney.edu.au (R.D. Müller)

Tel: +61 (0) 2 9036 6533; Fax: +61 (0) 2 9351 2442

Abstract

A multitude of observations suggest neotectonic deformation in and around India, but its causes and history is unknown. We use a 2 dimensional finite element model with heterogeneous elastic strengths in continental regions to model the regional stress field orientation and relative magnitudes since the Oligocene. The large-scale geological structure of India is embedded in our model by using published outlines of cratons, fold belts and basins, associated with estimates of their relative strengths, enabling the modelling of stress field deflections along interfaces between relatively strong and weak tectonic elements through time. At 33 Ma a roughly NNW-SSE oriented band of relatively high maximum horizontal compressive stress (S_{Hmax}) straddled India's west coast, while India's east coast and the adjacent Wharton Basin were characterized by relatively low intraplate stresses. Between 20 Ma and the present growing collisional boundary forces combined with maturing mid-ocean ridge flanks result in the establishment of an arcuate belt with anomalously high intraplate stress that stretches from India to the Wharton Basin, intersecting the continental shelf roughly orthogonally and crossing the 85° East and Ninetyeast ridges. This results in a compressive tectonic regime favouring folding and inversion northeast of the Godavari Graben on India's east coast, as observed in seismic reflection data, whereas no tectonic reactivation is observed on the continental margin further north, closer to the Mahanadi Graben, or further south. Our stress models account for these differences via spatial variations in modelled horizontal stress magnitudes and intersection angles between margin-paralleling pre-existing basement structures and the evolving Neogene stress field. The models further account for fracture zone strike-slip reactivation offshore Sumatra and lithospheric folding along India's west and southeast coast and can be used to estimate the onset of these deformation episodes to at least the Oligocene and Miocene, respectively.

1. Introduction

Diffuse plate boundary deformation in the equatorial Indian Ocean is well understood in the context of the fragmentation of the Indo-Australian Plate following India-Eurasia collision. The progressive collision between India and Eurasia since the Oligocene has produced the largest intra-oceanic fold and thrust belt on Earth (Royer and Gordon, 1997). Its effects on the progressive deformation of the Central Indian Basin (Bull et al., 2010; Krishna et al., 2009), the breakup of the Indo-Australian Plate into the Indian, Capricorn and Australian plates (DeMets et al., 2005; Gordon et al., 1998), the first-order plate-wide stress field (Cloetingh and Wortel, 1986; Coblentz et al., 1998) as well as the detailed Australian stress field evolution (Dyksterhuis and Müller, 2008; Müller et al., 2012) have been studied. Published seismic profiles document folding on the eastern Indian continental shelf west of the northern segment of the 85° East Ridge (Bastia et al., 2010; Radhakrishna et al., 2012), an observation not accounted for by current tectonic models. A variety of observations related to the evolution of intraplate deformation can be analysed in the context of current and past intraplate stresses. The present-day stress field of the central Indian Ocean has been studied extensively, revealing regional patterns of extension in the west versus compression in the east of the central Indian Basin, and illuminating the role of the Chagos-Laccadive and Ninetyeast ridges in controlling the style of deformation (Delescluse and Chamot-Rooke, 2007; Sager et al., 2013). There are sophisticated published models for understanding global plate driving forces and lithospheric stresses, either focussing on the effect of mantle forces (Steinberger et al., 2001), or both mantle forces, large-scale lithospheric structure and topography (Ghosh et al., 2013; Ghosh and Holt, 2012; Lithgow-Bertelloni and Guynn, 2004). However, these models are all confined to the present-day and have never been applied to the geological past. The reason for this is that various key model inputs and observations are not easy to quantify for the geological past. There is no global paleo-stress map for any time in the past. By the same token, we don't know paleotopography very well, a case in point being the Tibetan Plateau, where there are widely diverging interpretations of the evolution of Tibetan Plateau elevation, even at relatively recent times. In a recent review, Molnar et al. (2010) noted that the Tibetan Plateau elevation history cannot be quantified, but it seems likely that by 30 Ma a huge area north of Asia's pre-collisional southern margin extended from 20–25°N to nearly 40°N with a mean elevation perhaps as high as 1000 m. In the same year Song et al. (2010) estimated Tibetan Plateau elevation to have been at least 3000 m since even earlier times, i.e. the Eocene. These large uncertainties make it difficult to use paleo-elevation estimates in paleo-stress models. In addition sparse geological and geophysical observations need to be used to ground-truth paleo-stress models, such as folding and faulting visible in seismic reflection lines across sedimentary basins and margins (Bastia and Radhakrishna, 2012; Gombos et al., 1995), rock microstructures from outcrops (Letouzey, 1986; Sippel et al., 2010) and fracture systems in chalk (Duperret et al., 2012). The sparsity of these data, which are additionally not compiled in any database (unlike present-day stress data) imply that the generation and testing of sophisticated lithospheric stress models for the geological past is challenging, as some key boundary conditions like topography and mantle structure are not well known, and nor are there rich and spatially dense data available for model validation. For the Indian subcontinent and the surrounding ocean crust a diverse range of observations have been used to constrain the nature and timing of tectonic reactivation, ranging from the mapping and modelling of folding and faulting of ocean crust in the central Indian Basin (Krishna et al., 2009; Royer and Gordon, 1997), the mapping of river paleo-channels (Subrahmanya, 1996), using geologic, geomorphic, and tide-gauge data to detect lithospheric buckling (Bendick and

Bilham, 1999), measuring fault activity and slip rates (Banerjee et al., 2008; Clark and Bilham, 2008; McCalpin and Thakkar, 2003) and analysing Quaternary intraplate seismicity (Bilham et al., 2003) (Table 1). However, to date there are no published models of the intraplate stress evolution of the Indian subcontinent, nor for any other continent, with the exception of Australia (Müller et al., 2012). Modelling of the Australian paleo-stress field (Müller et al., 2012) has shown that if the horizontal continental stress field is strongly dominated by compressional edge forces, i.e. collisions and mid-ocean ridge forces, the first-order features of the stress field are well captured without including mantle forces or topography. A major problem with including mantle forces in paleostress models is our lack of knowledge of asthenospheric viscosity and its spatial and time-dependent variation, which is the main parameter governing how well mantle convection is coupled to a given plate or continent. This uncertainty is expressed in the great controversy over the influence of mantle convection and plume driving forces on the time-varying speed of the Indian Plate since the Late Cretaceous (Cande and Stegman, 2011; Kumar et al., 2007; van Hinsbergen et al., 2011), versus the effect of climate change (Iaffaldano et al., 2011) or changes in subduction geometry (Müller, 2007).

Despite the great uncertainties in paleo-stress field modelling, the sparsity of data and the simplicity of current modelling approaches, our motivation for exploring relatively simple paleo-stress models for India is the substantial interest in understanding the evolution of continental stress fields, for instance to unravel the formation and reactivation of structural hydrocarbon traps on the continental shelf (Bastia and Radhakrishna, 2012; Gombos et al., 1995) and for understanding the tectonic history of mobile belts and adjacent regions and their links with deep Earth resources.

Here we focus on modeling the evolution of India's paleo-stress field. We combine observations related to different time scales, using the world stress map database (years - 1000s of years) as well as structural reactivation and sediment folding visible in seismic reflection data (millions of years). Our study is focused on modeling the paleo-continental stress field, as opposed to building a detailed model for the present-day field. Our oceanic model lithosphere has a relatively simple structure, unlike the detailed models by Delescluse and Chamot-Rooke (2007) and Sager et al. (2013), which take into account the effect of aseismic ridges, seamount chains and other structural discontinuities on instantaneous deformation of the ocean crust. Our relatively simple models are not designed to compete with these more sophisticated plate deformation models for the present day. Instead our models are deliberately simplified in oceanic realms to allow us to restore now subducted ocean crust, whose detailed local structure is not known, and to primarily focus on modeling the past continental stress field. For paleo-stress field models the data available for model testing or validation are tiny in quantity and very different in character compared with the wealth and diversity of data constraining the present-day stress field (Heidbach et al., 2007). Tectonic reactivation through geological time is mainly reflected in faulting and folding preserved in basin and margin sediments, imaged by seismic reflection profiles. The model presented in this paper, designed to understand the paleo-stress field evolution of India, is the first of its kind; in addition to providing a first-order basis for understanding the nature and driving forces of structural reactivation in India and along its margins, it also provides an intriguing hint that the evolution of plate-driving forces and far-field stresses since the Miocene may allow us to better understand the concentration of intraplate stress south of Sumatra.

2. Model setup

We construct the first paleostress model for India by applying a well-established paleo-stress modelling methodology (Dyksterhuis et al., 2005a; Dyksterhuis and Müller, 2008; Dyksterhuis et al., 2005b) to model its lithospheric stress field and the surrounding oceanic crust for three time slices, the Late Oligocene (33 Ma), the early Miocene (20 Ma) and the present. These times were chosen because they represent tectonic events seen in India-Eurasia convergent rate graphs (Zahirovic et al., 2012). Paleostress modelling of the Australian continent has shown that both present and past stress fields can be well approximated by plate boundary stresses alone when the stress field is dominated by collisional forces, largely balanced by mid-ocean ridge forces (Müller et al., 2012). In these static paleostress models one side of the perimeter of a given plate needs to be kept fixed, and in our case we use the Tibetan Plateau. This means that instead of depending on the need to know the combination of forces actually acting on that side of the plate, including its topography, all other boundary forces acting on the plate are balanced by an equivalent force along the side that is being held fixed. The applied forces are optimised to best match present-day stress field data (Heidbach et al., 2007), and the optimised present-day model is used as a blueprint for paleo-stress models, which are set up using reconstructed plate geometries following Seton et al. (2012).

We reconstruct the plate boundary configuration and age-area distribution of ocean crust around Australia through time to obtain estimates for ridge push, slab pull and collisional forces acting on the Indo-Australian Plate since the early Cretaceous, following the methodology outlined in Dyksterhuis et al. (2005a; 2005b). In the case of the Indo-Australian Plate the dominant plate driving forces are the ridge push, slab pull and collisional forces originating at subduction and collision zones along the northern margin of the Indo-Australian Plate (Dyksterhuis et al., 2005a). These forces are averaged over a 100 km thick lithosphere, and modelled stress magnitudes represent the deviatoric stress from a lithostatic reference state.

Modelling the contemporary and paleo-stress regimes was carried out using the finite element method as implemented in ABAQUS. Plate boundary geometries were imported from the plate boundaries dataset PB2002 (Bird, 2003). The outlines of continental tectonic elements for India and Australia were imported from the USGS Geologic Provinces of the World dataset (Osmonson et al., 2000). We use a two dimensional, elastic model typically containing around 32,000 plane stress, triangular finite elements giving an average lateral mesh resolution of around 35km, using a linear elastic model rheology. The relative material strengths of individual tectonic provinces were implemented via the Young's moduli of the materials, with initial estimates for continental elements (cratons, fold belts and basins) taken from Dyksterhuis et al. (2005a). These Young's Modulus values are scaled 'effective' values, based upon the flexural rigidity estimates for Australia (Zuber et al., 1989), which we apply equivalently to similar terranes in India (Fig. S1, Table S1).

The use of the terms "strength", "strong", or "weak" here refer to relative stiffness or deformability of the lithosphere within an elastic regime (as governed by Young's modulus and Poisson's ratio), as opposed to some measure of the stress or stress differences that results in an onset of anelasticity. As we are constrained to (linearly) elastic behaviour, we have no consideration for any departure from that rheology. Due to limitations of the elastic method and the way in which material strengths are implemented in the modelling process (ie. by using an effective Young's modulus), the modelled σH magnitudes do not represent values with an accurate magnitude in an absolute sense, but rather represent relative magnitudes.

Initial boundary forces were assigned following Dyksterhuis et al. (2005a; 2005b) (Fig. S2, Table S2). However, the forces acting at subduction boundaries are not well understood, and differ at each individual subduction zone. Hence subduction zone forces are included as free parameters in the optimisation, whereas the mid-ocean ridge forces, which can be computed based on the age-area distribution of ocean floor (Müller et al., 2008a) remain fixed during optimisation. The Himalayan boundary was fixed to the model space edge to maintain equilibrium in the model. Plate geometries were projected into Cartesian space utilising a Lambert equal area projection that minimizes distortion of the model area. For a more in-depth account of the modelling process see Dyksterhuis et al. (2005a). World stress map (WSM) data (Heidbach et al., 2007; Zoback, 1992) (Fig. 1) were used to optimise plate driving forces and the model rheology. These data represent Maximum Principal Stress orientations (σ_{Hmax}), classed according to the quality A, B or C; with A being within +/-15°, B within +/-20°,and C within +/-25° (Zoback, 1992).

Instead of attempting to explicitly use paleotopography, which is not well known, as model input, we instead model the net forces acting on the Indian sub-continent along its northern boundary as a balanced response to all other forces applied to the model. Our models are far too simple for us to be able to interpret the resulting absolute stress magnitudes; therefore we restrict ourselves to interpreting the changes in maximum horizontal stress orientations through time, and major changes in the location of highly stressed lithospheric regions through time. These results are quite independent of the exact scaling of the equivalent collisional force along the fixed perimeter of our models.

3. Plate reconstructions, ridge push and slab pull forces through time

Using a global relative and absolute plate motion model (Müller et al., 2008a; Müller et al., 2008b) we created reconstructions of the geometry (Figs. S2, S3) and age-area distribution of the ocean floor of the Indo-Australian Plate region for the Early Miocene (20 Ma) and Late Oligocene (33 Ma). The optimum plate rheology values from the contemporary model were used in the reconstructed models. However there are two reconstructed areas, as parts of greater India and greater Papua New Guinea, which have now been destroyed through collisional processes. These areas were assigned the values of 'Himalayan foreland' region and 'Papua New Guinea', respectively (Table S1). The same methodology as used to calculate present-day mid-ocean ridge forces was applied to reconstructed plate assemblies, based on the reconstructed age-area distribution of the ocean floor (Müller et al., 2008b). Subduction zones around the Indo-Australian Plate have changed substantially throughout the Neogene. We use the previously established approach to estimate paleo-plate driving forces for subduction zones, by our present-day model inversion, using the approach outlined in Dyksterhuis and Müller (2005a) and Dyksterhuis et al. (2005b) (Tables S2 and S3). Despite relatively minor changes in mid-ocean ridge geometries since the Oligocene in our study area, the applied ridge push force is over 60 % smaller in the Oligocene than at present. This is because the expression "ridge push" is a misnomer, in the sense that the force which the mid-ocean ridge system exerts on the plate on either side of a given ridge arises due to the total area of elevated topography at mid-ocean ridges and their flanks relative to abyssal plains. The ridge push force corresponds to a distributed pressure gradient that acts normal to the strike of the mid-ocean ridge (Wilson, 1993), and is based on the age-area (and consequent depth-area) distribution of a given mid-ocean ridge flank, as opposed to the ridge alone pushing the plates apart. The force contribution from the subsiding and cooling oceanic lithosphere bordering a mid-ocean ridge is given by this relationship (Turcotte and Schubert, 2002):

$$F_{RP} = g\rho_{\mathrm{m}}\alpha_v \left(T_m - T_0\right)\left[1 + \frac{2}{\pi}\frac{\rho_m\alpha_v\left(T_m - T_0\right)}{\left(\rho_m - \rho_0\right)}\right]\kappa t$$

where gravity (g) is 10m/s^2, the densities of the mantle (ρ_m) and water (ρ_w) are 3300 kg/m^3 and 1000 kg/m^3 respectively, thermal diffusivity (κ) is 1 mm^2/s, the temperature difference between the mantle and the surface (T_m and T_0 respectively) is 1200 K, the thermal expansion coefficient (α_v) is 3 x 10^{-5}/K and t is the age of the lithosphere in seconds. In the Oligocene, most of the currently existing ridge flanks in the southeast Indian ocean did not yet exist, as seafloor spreading had been extremely slow until about 45 Ma (Müller et al., 2008b); therefore the ridge flank area contributing to "ridge push" was significantly smaller in the Oligocene compared to today.

The slab pull force originates from the negative buoyancy of the down-going dense oceanic lithosphere at subduction zones and is proportional to the excess mass of the cold slab in relation to the mass of the warmer displaced mantle (Spence, 1987). The force contribution can be given by the relationship (Turcotte and Schubert, 2002):

$$F_{SP} = \left(2\rho_m g\alpha_v b(T_c - T_0)\left(\frac{\kappa\lambda}{2\pi u_0}\right)^{1/2}\right) + \left(\frac{2(T_c - T_0)\gamma\Delta\rho_{os}}{\rho_m}\left(\frac{\kappa\lambda}{2\pi u_0}\right)^{1/2}\right)$$

where b = slab length, λ = 4000 km, u_0 = 50 mm/yr, γ = 4MPa/K, $\Delta\rho_{os}$ = 270 kg/m^3, with the remaining parameters identical to those in the equation used for ridge push.

For fast moving plates (5-10 cm/yr) the subducting slab attains a 'terminal velocity' where forces related to the negative buoyancy of the slab are balanced by viscous drag forces acting on the slab as it enters the mantle and the net force experienced by the horizontal plate is quite small (Forsyth and Uyeda, 1975). The amount of net force actually transferred to the horizontal plate, however, is still quite controversial. Schellart (2004) suggests as little as 8%-12% of slab pull force is transferred to the horizontal plate while Conrad and Lithgow-Bertelloni (2002) suggest as much as 70%-100% may be transmitted. We varied the magnitudes of plate driving forces acting on a given subduction zone segment over a range of $5x10^{8}$ N/m to $-5x10^{-8}$ N/m with best-fit force signs and magnitudes for our present-day model constrained by the resulting fit stress directions from the global stress database (Heidbach et al., 2007). The collisional boundary between the Indo-Australian and Eurasian plates at the Himalayas was modelled as a fixed boundary in the modelling process in order to maintain mechanical equilibrium for all times. In our model this boundary will still contribute forces to the resultant stress field of the plate; however, these forces are not imposed but obtained in the modelling process as a set of forces balancing all other forces applied to the model.

The overall stress pattern in our best-fit models is controlled by a balancing of mid-ocean ridge forces along the southern margin of the Indo-Australian Plate and collision at the northern boundary at the Himalayas and Papua New Guinea, as concluded by previous studies (Hillis et al., 1997). The exact contribution of slab pull to the motion of plates is theoretically a few times 10^{13} N m^{-1} (Coblentz et al., 1995). However, results from previous studies (Richardson, 1992) and our own modelling of the Indo-Australian stress field strongly indicate that the dominant driving forces acting on the Indo-Australian Plate are ridge and collisional forces, with forces acting at subduction boundaries mostly contributing a compressive force to the total Indo-Australian stress field. Copley et al. (2010) recently come to different conclusions with respect to the force balance for India, but their model was based on treating India as a separate plate, even though it is clearly strongly coupled to the Australian Plate, despite the existence of a diffuse plate deformation zone between them, and their modelling approach did not consider fitting stress field data.

4. Model Inversion

Inversion of model parameters was implemented by coupling the Nimrod/O optimisation software to ABAQUS model runs (Dyksterhuis and Müller, 2004). Nimrod/O can be set up to run an ABAQUS finite element model tied to Nimrod's non-linear optimisation process. Nimrod/O allows a user to specify the output variable to be minimized, which in our case corresponds to the residual σH misfit value, to optimise the overall fit between the stress models with observed data. Implementing ABAQUS in conjunction with Nimrod/O allowed for extensive exploration of the boundary force and material property parameter space through automated execution of thousands of models using intelligent optimisation techniques (Abramson et al., 2000; Lewis et al., 2003). Nimrod/O includes a number of alternative iterative automatic optimisation algorithms to search a parameter space for highly non-linear problems. It also enables parallel model runs, resulting in improved efficiency of the chosen optimisation method. For our palaeo-stress analysis the Simulated Annealing method van Laarhoven and Aarts (1987) embedded in Nimrod/O was chosen as it allows efficient escapes from local parameter space minima.

Nimrod/O contains algorithms for optimisation by minimising an objective function. The software package combines a number of different iterative automatic optimisation algorithms to intelligently search a parameter space for highly non-linear and over determined problems. It also enables parallel models runs, resulting in improved efficiency and intelligence of the standard optimisation methods. It further has the advantage that it is completely separate from a given forward model, and the objective function used. For our problem the simulated annealing method was chosen, as it allows an efficient escape from local parameter space minima (van Laarhoven and Aarts, 1987). This implementation included a preliminary testing of random starting points to evaluate the smoothness of the parameter space, and multiple random evaluations at each step.

A +/-0.5° latitude and longitude window was searched around each relevant WSM measurement (Fig. 1) and the mean taken of the residual between the observed and modelled principal stress field orientation. We found that the A residuals had a Gaussian distribution centred at ~15°, with outliers or 'noise' above 30°. The B class data had a similar distribution though slightly higher spread as expected. The C class data, however, had a near-uniform distribution from 0-90°. Hence we used a weighted mean function for assessing the goodness of fit of a given model to combined WSM data with differing quality: Objective function = (4*mean(A) + 3*mean(B) + 1*mean(C))/8.

As the number of unknown variables increases, there is a proportionally exponential growth in the complexity of the optimisation problem to be solved, which results in a more complex and sensitive solution space to explore. The computing time also increases exponentially as the parameter space is raised to higher dimensions. Hence steps were taken to reduce the number of variables, and place reasonable constraints on the bounds of their possible values. In the model the plate geometry and geometry of lithospheric tectonic elements is assumed to be correct, leaving rock strength and boundary forces to adjust. To further constrain the optimisation, we assume the Poisson's ratio (0.25) to be correct as it varies little (Christensen, 1996).

The initial estimate for equivalent Young's Moduli for lithospheric provinces were taken from Dyksterhuis et al. (2005b) who scaled flexural rigidity to a relative Young's Modulus by a linear constant. For the Indian continental Young's Moduli, a limit of +/-20% variation was set. Because mid-ocean ridge forces can be computed precisely given an age-area distribution of ridge flanks, the computed initial values were held constant. All other forces were set to an initial estimate as summarised in Tables S2 and S3 with bounds of +/- 20%. The best-fit values obtained via optimisation from the contemporary model were propagated into the paleo-models, but using reconstructed plate boundary geometries and computing ridge forces derived from reconstructed age-area distributions of ocean floor age.

5. Results

More than 10000 models were executed before converging on a best-fit present-day model (Fig. 1), which has a mean residual of 15° using A-quality stress data and ~30° over the weighted A, B and C WSM measurements, resulting in the refined plate boundary forces and model rheologies listed in Tables S1-3. To investigate the sensitivity of the model, the optimized solution was used to conduct an exhaustive search on the boundary forces only. The bounds of the search were set to +/- 10% of magnitude for a given optimized force. The resulting dataset of more than 2500 residual stress directions had a standard deviation of just 0.07°, illustrating that the model as a whole is relatively insensitive to precise scaling of boundary forces.   This justifies the use of approximate boundary forces for reconstructed models, which cannot be formally optimized against any given data set, given the scarcity of paleo-stress observations. WSM stress data at a given location may also be affected by localized deviations of the stress field, such as local faults, which are not considered in our model. The residual misfits in our optimized model may largely reflect such local stress field variations. All initial and optimized model parameters are listed in Tables S1-3.

Our model illustrates how the complex evolution of edge forces acting on the Indo-Australian plate boundaries through time can account for the spatial distribution of intraplate seismicity offshore Sumatra as well as non-seismogenic deformation along India's eastern margin. At 33 Ma a roughly NNW-SSE oriented band of relatively high maximum horizontal compressive stress (S_{Hmax}) straddled India's west coast, while India's east and the Wharton Basin were characterized by relatively low intraplate stresses (Figs. 2a and 3a). At 20 Ma the compressional belt crossing India widens substantially and propagates beyond the SE coast, while the Wharton Basin remains at low intraplate stress levels (Figs. 2b and 3b). Between 20 Ma and the present-day growing collisional boundary forces combined with maturing mid-ocean ridge flanks and increasing ridge push force result in the establishment of an arcuate belt with anomalously high intraplate stress that stretches from India to the Wharton Basin, intersecting the continental shelf and crossing the 85°East and Ninetyeast ridges (Figs. 2b, 2c, 3b and 3c).

6. Discussion

Lithospheric buckling

A combination of onshore geomorphological observations, potential field data and the distribution and type of earthquakes have led to the suggestion that large-scale buckling and/or fault reactivation of the Indian lithosphere may be occurring as a consequence of the India-Eurasia collision (Bendick and Bilham, 1999; Subrahmanya, 1996; Vita-Finzi, 2004, 2012). Here we use a recently published Bouguer gravity anomaly grid (Fig. 5) by Balmino et al. (2012) to test these hypotheses, in the context of our stress models. Lithospheric buckling is expected to cause Moho undulations which should be well expressed in Bouguer gravity anomalies. We also plot published structural trends over the EMAG2 magnetic anomaly map (Maus et al., 2009) (Fig. 6) in the expectation that prominent linear magnetic anomalies may reflect major crustal/lithospheric inhomogeneities and/or intrusive bodies that may focus buckling in particular regions. Five WSW-ENE oriented fold axes along the southwest coast of India interpreted by Bendick and Bilham (1999), related to inferred buckling at wavelengths of about 200 km (Fig. 5), do not coincide with clear linear Bouguer gravity anomaly features with the exception of the axis located around 12°N, which is also located on the edge of a magnetic anomaly high to the north of the inferred fold axis (Fig. 6). This fold axis is also located close to the roughly east-west striking Mulki-Pulikat Lake Axis (Figs. 5 and 6) which separates northeast from southeast flowing rivers (Subrahmanya, 1996). All fold axes interpreted by Bendick and Bilham (1999) are sub-parallel with linear magnetic anomaly features (Fig. 6) and roughly orthogonal to our modelled current and paleo-stress S_{Hmax} directions. Therefore, these interpretations appear plausible even though not all of these features are expressed in Bouguer gravity anomalies.

The Bouguer anomaly map also reveals a series of sub-parallel NE-SW striking undulations with wavelengths of roughly 100 km in the southeastern region of India (Fig. 7), part of the "southern granulites" province (Figs. 2, 5). Since the directions of these linear Bouguer anomalies are orthogonal to the regional maximum horizontal stress field, which has persisted throughout the Neogene, we suggest that most of these structural trends likely reflect lithospheric folds formed in response to the regional NW-SE oriented maximum horizontal stress. These features are parallel to undulations in a previous isostatic gravity map used by Subrahmanya (1996) together with geological data to infer lithospheric buckling in the region. The northeasternmost extension of these gravity undulations is also associated with a group of large earthquakes (Fig. 5). The observed wavelengths are typical of lithospheric folding in relatively warm lithosphere (Burg and Podladchikov, 1999). This observation is consistent with the relatively high regional mantle heat flow modelled for parts of the Southern Granulite Province of 23–32 mW m^{-2}, contrasting with significantly lower mantle heatflow of 11–16 mW m^{-2} in the Archaean Dharwar greenstone-granite-gneiss province further north (Ray et al., 2003), where Bouguer gravity anomalies do not suggest short-wavelength lithospheric folding (Fig. 5). Our paleo-stress models suggest that the folds interpreted by Bendick and Bilham (1999) along the west coast of India may be as old as 33 Ma, as our models imply maximum horizontal stress directions orthogonal to these features with relatively high amplitudes since 33 Ma. In contrast, our model suggest that the southeastern granulite province folds are not older than 20 Ma. Even though our 33 Ma model exhibits similar S_{Hmax} orientations to the younger model times, the S_{Hmax} amplitudes were extremely small prior to 20 Ma (Fig. 2).

Continental shelf tectonic reactivation

The eastern continental shelf of India can be considered as two units, one paralleling the ~N-S trending coastline (south of 16°N, including the Godavari Graben) and another parallelling a NE-SW trend of the coastline (north of 16°N and between Godavari and Mahanadi grabens). The modelled azimuth of the maximum horizontal stress is orthogonal to the margin within the NE-SW striking shelf segment between the Godavari and Mahanadi grabens combined with relatively high horizontal stress magnitudes. This region corresponds to the basement-involving folds seen only in profiles P3 and P5 (Fig. 4), but not in profile P2 further north and profile P6 further south (Bastia and Radhakrishna, 2012). In the ~N-S trending continental margin unit, although the maximum horizontal stress magnitude is quite high here as well, the intersection angle of the stress field relative to the strike of the continental shelf is not orthogonal, but around ~45°, making this region more prone to strike-slip reactivation than folding, explaining the absence of major folds in profile P6. The absence of any major tectonic reactivation along profile P2 reflects the relatively low present-day horizontal stress magnitudes along this margin segment (Fig. 2).

At present day the highly stressed belt crossing India widens substantially, accompanied by increased horizontal stress magnitudes (Fig. 2c). Along the eastern margin of India this highly stressed band is split into two strands by the rheologically weak Godavari Graben and limited in extent towards the northeast by the Mahanadi Graben (Fig. 2c). S_{Hmax} orientations at both model times are roughly parallel to the western margin of India, thus limiting the likelihood of tectonic reactivation of rift-related faults there. In contrast, the S_{Hmax} orientations straddling the eastern margin of India intersect the continental shelf roughly orthogonally, between the Godavari and Mahanadi grabens, resulting in a compressive tectonic regime orthogonal to rift-related faults (Fig. 2c). This causes a tectonic regime favouring folding and inversion northeast of the Godavari Graben on India's east coast, as observed in seismic reflection data west of the northern portion of the 85° East Ridge (Bastia et al., 2010; Radhakrishna et al., 2012). Bastia et al.'s (2010) profile 5 (see Fig. 2c for location) intersects the Krishna-Godavari Basin and displays distinct folding at wavelengths of the order of 10 km of most of the sedimentary section along the foot of the continental slope; however the "shale bulge" folds are most visible in the Cenozoic section because of a distinct set of high-amplitude seismic reflections characterizing this part of the section (Radhakrishna et al., 2012) (Fig. 4b). Their profile 3 intersects the Visakhapatnam Bay Basin (Fig. 2c) and exhibits similar folds along the foot of the continental slope (Fig. 4a). In both cases the folds are centred on basement faults or highs. Our paleo-stress models suggest that this episode of folding occurred some time between 20 Ma and the present, when the NW-SE oriented band of high-magnitude maximum horizontal stress propagated southeastward onto the continental shelf northeast of the Godavari Graben, as observed on the present-day stress map for India (Fig. 2c).

It is important to recognise that such regional tectonic reactivation is not included in the global strain rate map of Kreemer et al. (2003). This map is entirely focussed on deformation adjacent to plate boundaries. In contrast, taking Australia as an example, there are several intracontinental regions, including the Adelaide fold belt and the Bass Strait, in which very well documented, severe intraplate deformation is taking place today (Hillis et al., 2008). Along the Adelaide fold belt this reactivation is associated with pronounced inversion and Neogene uplift of up to 1-2 km (Dyksterhuis and Müller, 2008; Holford et al., 2011). This region of major intraplate deformation is omitted in Kreemer et al's (2003) global strain rate map. Therefore there is no surprise that other regions of somewhat less severe intraplate deformation are equally omitted from this map, considering that Kreemer et al.'s (2003) map is focussed on deformation along active plate boundaries, not passive margins or other regions of rheological weakness within continental areas. Therefore the assimilation of geological data into current and paleo-stress maps plays an important role in highlighting additional areas of intraplate deformation.

The seismic reflection data we use here to ground-truth our model clearly show basement-involved folding and faulting in the region coinciding with a current horizontal stress maximum with maximum horizontal stress orientations roughly orthogonal to the strike of the margin (Figs. 4a, 4b). The fact that folding of the sedimentary succession can be traced all the way to basement steps excludes an interpretation of the features seen in the seismic data as slumping of sediments down the continental slope. In addition, the deformation seen here on profiles P3 and P5 is extremely similar to that well-documented on the northwest shelf of Australia in the Browse Basin (Müller et al., 2012; Struckmeyer et al., 1998), which is also associated with relatively old Early Cretaceous ocean floor, whereas we interpret the densely spaced subvertical faults visible on profile P6 as analogous to strike-slip and en-echelon faults found on Australia's Northwest shelf in an oblique compressional tectonic regime (De Ruig et al., 2000; Shuster et al., 1998).

The onset of deformation between the India and Capricorn plates in the Central Indian Basin has recently been estimated as 15.4–13.9 Ma from a combination of seismic stratigraphy and plate kinematics, with a sharp increase in fault activity at 8–7.5 Ma (Bull et al., 2010). Seismic profile 3 from Bastia et al. (2010) (Fig. 4b) illustrates that the top Miocene is similarly folded to deeper parts of the Cenozoic sequence, e.g. the Top Eocene, whereas the overlying Pliocene sequence is only gently folded. This indicates that this folding event occurred some time around the latest Miocene, and given the observed 8-7.5 Ma major increase in fault activity in the Central Indian Basin (Bull et al., 2010) it is likely that the propagation of increased maximum horizontal stresses onto this region of the continental margin as modelled for the present (Fig. 2c) occurred contemporaneously around this time.

The present-day horizontal stress field magnitudes exhibit a ~500km wide circular maximum offshore western Sumatra, intersecting three large-offset fracture zones at roughly 45°, favouring fracture zone strike-slip reactivation relatively close to the trench as expressed in the magnitude 8.6 and 8.2 events in April 2012, the largest oceanic strike-slip event in the instrumental record (Fig. 3c) (Delescluse et al., 2012; Yue et al., 2012). The post-20 Ma growth of trench-parallel horizontal stress magnitudes in oceanic domain results in another highly stressed band of ocean floor offshore eastern Sumatra and Java (Fig. 3c). However, most of it does not intersect major fracture zones, and therefore does not lead to great earthquake clusters. This difference is related to observations made by Deplus et al. (1998), who compared the mode of seafloor deformation east and west of the Ninetyeast Ridge, and noted that east of the ridge the presence of numerous fracture zones (Fig. 3c) interacts with the regional stress field to cause north-south strike-slip fault reactivation along these lines of tectonic weakness. In contrast, the region west of the Ninetyeast Ridge, where the maximum horizontal stress orientations are similar (Fig. 3c), but where fracture zones are more sparse, the seafloor deforms by folding and reverse faulting (Deplus et al., 1998). The latter regional pattern of deformation is not associated with great earthquakes (Fig. 3c), because a lower compressive stress magnitude compared to the region east of the Ninetyeast Ridge is paired with a lack of fossil fracture zones to be reactivated. The scarcity of major fracture zones south of eastern Sumatra and Java (Fig. 3c) equivalently prevents widespread strike-slip reactivation of fossil fracture zones here (with one exception being the Investigator Fracture Zone (Abercrombie et al., 2003)), whereas the tectonic niche environment southwest of Sumatra provides a unique coincidence of a regional compressive stress field intersecting three large-offset fracture zones at an ideal angle (~45°) for causing a regional cluster of large magnitude strike-slip earthquakes.

7. Conclusions

Our models represent the first set of paleo-stress models for India and the surrounding margin and ocean crust. Despite their simplicity, our paleo-stress models capture some first order features of the regional horizontal stress field evolution. They capture the effect of the progression from the initial “soft” collision between India and Eurasia to the present, mature collision state on the regional lithospheric stress field, and the modulation of stress magnitudes and directions by the geometry and strength of relatively weaker and stronger lithospheric elements including cratons, basins and fold belts. Even though western India was subject to relatively high horizontal stress during the soft collision, the propagation of anomalously high intraplate stress across the east coast of India and into the Central Indian Basin, reaching two maxima offshore Sumatra and Java, only occurred between 20 Ma and the present. Our model accounts for the occurrence of folding along the west and southeast coast of India as well along two segments of India's eastern continental margin, north and south of the Godavari Graben, respectively, and the lack of any major tectonic reactivation along the continental margin close to the Mahanadi Graben, reflecting the spatial differences in horizontal stress magnitudes and the intersection angle between the maximum horizontal stress directions and the strike of the margin, and thus the strike of margin-parallel tectonic basement fabric.

Our model also provides an explanation for the peculiar clustering of large earthquakes in the northern Wharton Basin, including the intraplate magnitude 8.6 and 8.2 events in April 2012, the largest oceanic intraplate earthquake in the instrumental record. The region represents a unique tectonic niche where three major fracture zones intersect an intraplate horizontal stress maximum at roughly 45°. A similar, more extensive stress maximum is modelled further east offshore Java, but it does not coincide with a large-offset fracture zone cluster, thus providing only few opportunities strike-slip reactivation of lithospheric weaknesses.

Our basic 2D model could be improved in many ways, for instance by using a depth-dependent rheology of the lithosphere, by attempting to include paleo-topography, and considering its uncertainties, by further exploring the parameter space of plate boundary forces through time, by including a more heterogeneous and realistic structure of the oceanic lithosphere and by compiling more observations constraining tectonic reactivation through time that could be used to further test paleo-stress models. However, considering that our relatively simple approach represents the first attempt at modelling the stress field history of India and its surrounds, we believe that our model has revealed some key first-order features of the regional paleo-stress field evolution, which will prove to be a useful reference model for future studies. In addition, our regional paleo-stress model data are freely downloadable from http://www.earthbyte.org/resources.html, making it easy to overlay other data over these models in a geographic information system and also potentially use them for assessing the regional risk of the breaching of hydrocarbon traps through time.

Acknowledgments

We thank S. Dyksterhuis for establishing the ABAQUS model setup and optimisation methodology, and we acknowledge J. Knight's help with refining the optimisation methodology. VY and MS are grateful to the Director, CSIR-National Institute of Oceanography (CSIR-NIO, Goa) for permission to publish this paper. We are grateful to M. Radhakrishna for providing us with high resolution images of published figures. We also thank M. Radhakrishna and three anonymous reviewers for helping to improve the paper significantly. We gratefully acknowledge the funding support received from Department of Science and Technology (DST), Govt. of India and Department of Innovation, Industry, Science and Research (DIISR), Govt. of Australia under an Australia-India Strategic Research Fund (AISRF) grant. A part of this work was carried out by MS as Junior Research Fellow of the University Grants Commission, New Delhi. RDM was supported by ARC grant FL0992245. Figures 1-3 and 5-7 were created with the GMT software (Wessel and Smith, 1995). This is NIO contribution number xxxx.

References

Abercrombie, R.E., Antolik, M., Ekström, G., 2003. The June 2000 Mw 7.9 earthquakes south of Sumatra: Deformation in the India–Australia Plate. Journal of Geophysical Research 108, 2018, doi:2010.1029/2001JB000674.

Abramson, D., Lewis, A., Peachy, T., 2000. Nimrod/O: A Tool for Automatic Design Optimization, The 4th International Conference on Algorithms & Architectures for Parallel Processing (ICA3PP 2000), Hong Kong, 11 - 13 December.

Balmino, G., Vales, N., Bonvalot, S., Briais, A., 2012. Spherical harmonic modelling to ultra-high degree of Bouguer and isostatic anomalies. Journal of Geodesy 86, 499-520.

Banerjee, P., Bürgmann, R., Nagarajan, B., Apel, E., 2008. Intraplate deformation of the Indian subcontinent. Geophysical Research Letters 35, L18301, doi: 10.1029/2008GL035468.

Bastia, R., Radhakrishna, M., 2012. Basin evolution & petroleum prospectivity of the Continental margins of India Elsevier.

Bastia, R., Radhakrishna, M., Srinivas, T., Nayak, S., Nathaniel, D.M., Biswal, T.K., 2010. Structural and tectonic interpretation of geophysical data along the Eastern Continental Margin of India with special reference to the deep water petroliferous basins. Journal of Asian Earth Sciences 39, 608-619.

Bendick, R., Bilham, R., 1999. Search for buckling of the southwest Indian coast related to Himalayan collision, Special Paper - Geological Society of America, pp. 313-321.

Bhattacharya, G., Subrahmanyam, V., 1986. Extension of the Narmada—Son lineament on the continental margin off Saurashtra, Western India as obtained from magnetic measurements. Marine Geophysical Researches 8, 329-344.

Bilham, R., Bendick, R., Wallace, K., 2003. Flexure of the Indian plate and intraplate earthquakes. Proceedings of Indian Academy of Science (Earth and Planetary Science) 112, 315-329.

Bird, P., 2003. An updated digital model of plate boundaries. Geochemistry, Geophysics, Geosystems 4, 1027, doi:1010.1029/2001GC000252.

Biswas, S., 1982. Rift basins in western margin of India and their hydrocarbon prospects with special reference to Kutch basin. American Association of Petroleum Geologists Bulletin 66, 1497-1513.

Bull, J., DeMets, C., Krishna, K., Sanderson, D., Merkouriev, S., 2010. Reconciling plate kinematic and seismic estimates of lithospheric convergence in the central Indian Ocean. Geology 38, 307-310.

Burg, J.-P., Podladchikov, Y., 1999. Lithospheric scale folding: numerical modelling and application to the Himalayan syntaxes. International Journal of Earth Sciences 88, 190-200.

Cande, S.C., Stegman, D.R., 2011. Indian and African plate motions driven by the push force of the Reunion plume head. Nature 475, 47-52.

Christensen, N.I., 1996. Poisson's ratio and crustal seismology. Journal of Geophysical Research 101, 3139-3156.

Clark, M.K., Bilham, R., 2008. Miocene rise of the Shillong Plateau and the beginning of the end of the Eastern Himalaya. Earth and Planetary Science Letters 269, 337-351.

Cloetingh, S., Wortel, R., 1986. Stress in the Indo-Australian Plate. Tectonophysics 132, 49-67.

Coblentz, D.D., Sandiford, M., Richardson, R.M., Zhou, S.H., Hillis, R., 1995. The Origins of the Intraplate Stress Field in Continental Australia. Earth and Planetary Science Letters 133, 299-309.

Coblentz, D.D., Zhou, S.H., Hillis, R.R., Richardson, R.M., Sandiford, M., 1998. Topography, Boundary Forces, and the Indo-Australian Intraplate Stress Field. Journal of Geophysical Research 103, 919-931.

Conrad, C., Lithgow-Bertelloni, C., 2002. How mantle slabs drive plate tectonics. Science 298, 207-209.

Copley, A., Avouac, J.P., Royer, J.Y., 2010. India-Asia collision and the Cenozoic slowdown of the Indian plate: Implications for the forces driving plate motions. Journal of Geophysical Research: Solid Earth 115, doi:10.1029/2009JB006634.

De Ruig, M., Trupp, M., Bishop, D., Kuek, D., Castillo, D., 2000. Fault architecture and the mechanics of fault reactivation in the Nancar Trough/Laminaria area of the Timor Sea, Northern Australia. The APPEA Journal 40, 174-193.

Delescluse, M., Chamot-Rooke, N., Cattin, R., Fleitout, L., Trubienko, O., Vigny, C., 2012. April 2012 intra-oceanic seismicity off Sumatra boosted by the Banda-Aceh megathrust. Nature 490, 240-244.

Delescluse, M., Chamot-Rooke, N., 2007. Instantaneous deformation and kinematics of the India–Australia Plate. Geophysical Journal International 168, 818-842.

DeMets, C., Gordon, R.G., Royer, J.Y., 2005. Motion between the Indian, Capricorn and Somalian plates since 20 Ma: implications for the timing and magnitude of distributed lithospheric deformation in the equatorial Indian ocean. Geophysical Journal International 161, 445-468.

Deplus, C., Diament, M., Hébert, H., Bertrand, G., Dominguez, S., Dubois, J., Malod, J., Patriat, P., Pontoise, B., Sibilla, J.-J., 1998. Direct evidence of active deformation in the eastern Indian oceanic plate. Geology 26, 131-134.

Duperret, A., Vandycke, S., Mortimore, R.N., Genter, A., 2012. How plate tectonics is recorded in chalk deposits along the eastern English Channel in Normandy (France) and Sussex (UK). Tectonophysics 581, 163-181.

Dyksterhuis, S., Albert, R.A., Müller, D., 2005a. Finite element modelling of intraplate stress using ABAQUS™. Computers and Geosciences 31, 297-307.

Dyksterhuis, S., Müller, D., 2004. Modelling the contemporary and palaeo stress field of Australia using finite-element modelling with automatic optimisation. Exploration Geophysics 35, 236-241.

Dyksterhuis, S., Müller, R.D., 2008. Cause and evolution of intraplate orogeny in Australia. Geology 36, 495-498.

Dyksterhuis, S., Müller, R.D., Albert, R.A., 2005b. Palaeo-stress field evolution of the Australian continent since the Eocene. Journal of Geophysical Research 110, B05102 doi:05110.01029/02003JB002728.

Dziewonski, A.M., Chou, T.-A., Woodhouse, J.H., 1981. Determination of earthquake source parameters from waveform data for studies of global and regional seismicity. Journal of Geophysical Research 86, 2825-2852.

Ekström, G., Nettles, M., Dziewonski, A.M., 2012. The global CMT project 2004-2010: Centroid-moment tensors for 13,017 earthquakes. Physics of the Earth and Planetary Science Interior 200-201, 1-9.

Forsyth, F., Uyeda, S., 1975. On the Relative Importance of the Driving Forces of Plate Motion. Geophysical Journal of the Royal Astronomical Society 43, 163-200.

Ghosh, A., Holt, W., Wen, L., 2013. Predicting the lithospheric stress field and plate motions by joint modeling of lithosphere and mantle dynamics. Journal of Geophysical Research: Solid Earth 118, 346-368.

Ghosh, A., Holt, W.E., 2012. Plate motions and stresses from global dynamic models. Science 335, 838-843.

Gombos, A.M., Powell, W.G., Norton, I.O., 1995. The tectonic evolution of western India and its impact on hydrocarbon occurrences: An overview. Sedimentary Geology 96, 119-129.

Gordon, R.G., Demets, C., Royer, J.Y., 1998. Evidence For Long-Term Diffuse Deformation of the Lithosphere of the Equatorial Indian Ocean. Nature 395, 370-374.

Gowd, T., Srirama Rao, S., Chary, K., 1996. Stress field and seismicity in the Indian shield: effects of the collision between India and Eurasia. Pure and Applied Geophysics 146, 503-531.

Heidbach, O., Reinecker, J., Tingay, M., Müller, B., Sperner, B., Fuchs, K., Wenzel, F., 2007. Plate boundary forces are not enough: Second- and third-order stress patterns highlighted in the World Stress Map database. Tectonics 26, doi:10.1029/2007TC002133.

Hillis, R., Sandiford, M., Coblentz, D., Zhou, S., 1997. Modelling the Contemporary Stress Field and its Implications for Hydrocarbon Exploration. Exploration Geophysics 28, 88-93.

Hillis, R.R., Sandiford, M., Reynolds, S.D., Quigley, M.C., 2008. Present-day stresses, seismicity and Neogene-to-Recent tectonics of Australia's 'passive'margins: intraplate deformation controlled by plate boundary forces. Geological Society, London, Special Publications 306, 71-90.

Holford, S.P., Hillis, R.R., Hand, M., Sandiford, M., 2011. Thermal weakening localizes intraplate deformation along the southern Australian continental margin. Earth and Planetary Science Letters 305, 207-214.

Iaffaldano, G., Husson, L., Bunge, H.-P., 2011. Monsoon speeds up Indian plate motion. Earth and Planetary Science Letters 304, 503-510.

Kreemer, C., Holt, W.E., Haines, A.J., 2003. An integrated global model of present-day plate motions and plate boundary deformation. Geophysical Journal International 154, 8-34.

Krishna, K., Bull, J., Scrutton, R., 2009. Early (pre–8 Ma) fault activity and temporal strain accumulation in the central Indian Ocean. Geology 37, 227-230.

Kumar, P., Yuan, X., Kumar, M.R., Kind, R., Li, X., Chadha, R., 2007. The rapid drift of the Indian tectonic plate. Nature 449, 894-897.

Letouzey, J., 1986. Cenozoic paleo-stress pattern in the Alpine foreland and structural interpretation in a platform basin. Tectonophysics 132, 215-231.

Lewis, A., Abramson, D., Peachy, T., 2003. An Evolutionary Programming Algorithm for Automatic Engineering Design, Fifth International Conference on Parallel Processing and Applied Mathematics, Czestochowa, Poland.

Lithgow-Bertelloni, C., Guynn, J.H., 2004. Origin of the lithospheric stress field. Journal of Geophysical Research 109, 1-32.

Matthews, K.J., Müller, R.D., Wessel, P., Whittaker, J.M., 2011. The tectonic fabric of the ocean basins. Journal of Geophysical Research 116, B12109, 1-28.

Maus, S., Barckhausen, U., Berkenbosch, H., Bournas, N., Brozena, J., Childers, v., Dostaler, F., Fairhead, J.D., Finn, C., von Frese, R.R.B., Gaina, C., Golynsky, S., Kucks, R., Luhr, H., Milligan, P., Mogren, S., Muller, R.D., Olesen, O., Puikington, M., Saltus, R., Schreckenberger, B., Thebault, E., Tontini, F.C., 2009. EMAG2: A 2–arc min resolution Earth Magnetic Anomaly Grid compiled from satellite, airborne, and marine magnetic measurements. Geochemistry Geophysics Geosystems 10, Q08005, doi:10.1029/2009GC002471.

McCalpin, J.P., Thakkar, M.G., 2003. 2001 Bhuj-Kachchh earthquake: surface faulting and its relation with neotectonics and regional structures, Gujarat, Western India. Annals of Geophysics 46, 937-956.

Mitra, N., 1994. Tensile Resurgence along fossil sutures: a hypothesis on the evolution of Gondwana Basins of Peninsular India, In: Biswas, S.K. (Ed.), Proceedings, 2nd Symposium on Petroliferous basins of India. Indian Petroleum Publishers, Dehradun, pp. 55-62.

Molnar, P., Boos, W.R., Battisti, D.S., 2010. Orographic controls on climate and paleoclimate of Asia: thermal and mechanical roles for the Tibetan Plateau. Annual Review of Earth and Planetary Sciences 38, 77-102.

Müller, R.D., 2007. Earth science - An Indian cheetah. Nature 449, 795-797.

Müller, R.D., Dyksterhuis, S., Rey, P., 2012. Australian paleo-stress fields and tectonic reactivation over the past 100 Ma. Australian Journal of Earth Sciences 59, 13-28.

Müller, R.D., Sdrolias, M., Gaina, C., Roest, W.R., 2008a. Age, spreading rates, and spreading asymmetry of the world's ocean crust. Geochemistry, Geophysics, Geosystems 9, 1-19.

Müller, R.D., Sdrolias, M., Gaina, C., Steinberger, B., Heine, C., 2008b. Long-term sea level fluctuations driven by ocean basin dynamics. Science 319, 1357-1362.

Osmonson, L., Persits, F., Steinhouer, D., Klett, T., 2000. Geologic provinces of the world, US Geological Survey (USGS), Denver, CO.

Radhakrishna, M., Twinkle, D., Nayak, S., Bastia, R., Rao, G.S., 2012. Crustal structure and rift architecture across the Krishna-Godavari Basin in the central Eastern Continental Margin of India based on analysis of gravity and seismic data. Marine and Petroleum Geology 37, 129-146.

Ray, L., Kumar, P.S., Reddy, G., Roy, S., Rao, G., Srinivasan, R., Rao, R., 2003. High mantle heat flow in a Precambrian granulite province: Evidence from southern India. Journal of Geophysical Research: Solid Earth (1978–2012) 108.

Richardson, R.M., 1992. Ridge forces, absolute plate motions, and the intraplate stress field. Journal of Geophysical Research 97, 11739-11748.

Royer, J.-Y., Gordon, R.G., 1997. The motion and boundary between the Capricorn and Australian plates. Science 277, 1268-1274.

Sager, W., Bull, J., Krishna, K., 2013. Active faulting on the Ninetyeast Ridge and its relation to deformation of the Indo-Australian plate. Journal of Geophysical Research 118, 4648-4668.

Schellart, W.P., 2004. Quantifying the net slab pull force as a driving mechanism for plate tectonics. Geophysical Research Letters 31, doi:10.1029/2004GL019528.

Seton, M., Müller, R., Zahirovic, S., Gaina, C., Torsvik, T., Shephard, G., Talsma, A., Gurnis, M., Turner, M., Chandler, M., 2012. Global continental and ocean basin reconstructions since 200 Ma. Earth-Science Reviews 113, 212-270.

Shuster, M., Eaton, S., Wakefield, L., Kloosterman, H., 1998. Neogene tectonics, greater Timor Sea, offshore Australia: implications for trap risk. The APPEA Journal 38, 351-379.

Sippel, J., Saintot, A., Heeremans, M., Scheck-Wenderoth, M., 2010. Paleostress field reconstruction in the Oslo region. Marine and Petroleum Geology 27, 682-708.

Song, X.-Y., Spicer, R.A., Yang, J., Yao, Y.-F., Li, C.-S., 2010. Pollen evidence for an Eocene to Miocene elevation of central southern Tibet predating the rise of the High Himalaya. Palaeogeography, Palaeoclimatology, Palaeoecology 297, 159-168.

Spence, W., 1987. Slab Pull and the Seismotectonics of Subducting Lithosphere. Reviews of Geophysics 25, 55-69.

Steinberger, B., Schmeling, H., Marquart, G., 2001. Large-scale lithospheric stress field and topography induced by global mantle convection. Earth and Planetary Science Letters 186, 75-91.

Struckmeyer, H.I.M., Blevin, J.E., Sayers, J., Totterdell, J.M., Baxter, K., Cathro, D.L., 1998. Structural evolution of the Browse basin, North West Shelf: new concepts from deep-seismic data, In: Purcell, P.G.R.R. (Ed.), The Sedimetary Basins of Western Australia 2: Proceedings of Petroleum Exploration Society of Australia Symposium. Petroleum Exploration Society of Australia, Perth, WA, pp. 345-367.

Subrahmanya, K.R., 1996. Active intraplate deformation in south India. Tectonophysics 262, 231-241.

Turcotte, D.L., Schubert, G., 2002. Geodynamics, 2nd ed. Cambridge University Press, New York.

van Hinsbergen, D.J., Steinberger, B., Doubrovine, P.V., Gassmöller, R., 2011. Acceleration and deceleration of India-Asia convergence since the Cretaceous: Roles of mantle plumes and continental collision. Journal of Geophysical Research: Solid Earth 116, B06101, doi: 06110.01029/02010JB008051.

van Laarhoven, P.J., Aarts, E.H., 1987. Simulated annealing, Simulated Annealing: Theory and Applications. Springer Netherlands, pp. 7-15.

Vita-Finzi, C., 2004. Buckle-controlled seismogenic faulting in peninsular India. Quaternary Science Reviews 23, 2405-2412.

Vita-Finzi, C., 2012. River history and tectonics. Philosophical Transactions of the Royal Society A: Mathematical, Physical and Engineering Sciences 370, 2173-2192.

Wessel, P., Smith, W.H., 1995. New version of the generic mapping tools. Eos Transactions, American Geophysical Union 76, 329.

Wilson, M., 1993. Plate-Moving Mechanisms - Constraints and Controversies. Journal of the Geological Society 150, 923-926.

Yue, H., Lay, T., Koper, K.D., 2012. En echelon and orthogonal fault ruptures of the 11 April 2012 great intraplate earthquakes. Nature 490, 245-249.

Zahirovic, S., Müller, R.D., Seton, M., Flament, N., Gurnis, M., Whittaker, J., 2012. Insights on the kinematics of the India-Eurasia collision from global geodynamic models. Geochemistry Geophysics Geosystems 13, Q04W11.

Zoback, M., 1992. First- and Second-Order Patterns of Stress in the Lithosphere: The World Stress Map Project. Journal of Geophysical Research 97, 11,703-711,728.

Zuber, M.T., Bechtel, T.D., Forsyth, D.W., 1989. Effective elastic thickness of the lithosphere and mechanisms of isostatic compensation in Australia. Journal of Geophysical Research 94, 9353-9367.

Tectonic event	Timing	Evidence	Reference
Intraplate deformation in Central Indian Basin	mid-Miocene	Large-scale folding & faulting	[1], [2]
Quaternary Seismicity	Quaternary	Large magnitude earthquakes (eg. Bhuj, Latur, Koyna)	[3]
Uplift of southern Indian peninsula	Quaternary	Migration of paleo-channels, seaward shift of bathymetry contours	[4]
Rise of Shillong Plateau	Miocene	Acceleration of fault slip rates along the Shillong Plateau	[5], [6]
Tectonic uplift in Kachchh	Early Quaternary	Activities along E-W trending Katrol Hill Fault	[7]
Tectonic uplift in Kachchh	Late Pleistocene	Activities of transverse strike-slip faults	[7]
Lithospheric buckling along southwest coast of India (200 km wavelength)	Quaternary	Geologic, geomorphic, and tide-gauge data	[8]

Table 1. Chronology of Neogene tectonic events on and around the Indian subcontinent. [1] (Royer and Gordon, 1997); [2] (Krishna et al., 2009); [3] (Bilham et al., 2003); [4] (Subrahmanya, 1996); [5] (Banerjee et al., 2008); [6] (Clark and Bilham, 2008); [7] (McCalpin and Thakkar, 2003); [8] (Bendick and Bilham, 1999)

Figure captions

Figure 1. Modelled present-day maximum horizontal stress magnitudes (following the convention that compression is positive) and directions (shown by thin black bars) for the Indo-Australian plate. Stress orientation data are from the world stress map database, with category A (purple) and B (blue) data colour coded. Stress data with quality less than B are omitted from this map to improve its readability – however, C-quality data were included in our model. SUM: Sumatra

Figure 2. Modeled maximum horizontal stress magnitudes and directions for India for the late Oligocene (33 Ma) (a), Early Miocene (20 Ma) (b) and the present (c). Plotting conventions as in Fig. 1. Outlines of major seamount chains are shown as thin light grey lines, and boundaries between continental and oceanic crust (Müller et al., 2008a) as thick grey lines. Major faults, rifts and other structural and tectonic trends are compiled from Biswas (1982), Bhattacharya and Subrahmanyam (1986) and Mitra (1994) and plotted as thick black lines. The thick dotted lines represent locations of seismic sections presented in Figure 4. The red lines represent fold axes inferred to have formed due to neotectonic events of uplift and subsidence caused by buckling of lithosphere (Bendick and Bilham, 1999). The dashed magenta line represents the Mulki-Pulikat Lake Axis (Subrahmanya, 1996), which separates northeast flowing rivers from southeast flowing rivers. NSL: Narmada-Son Lineament; GG: Godavari Graben; MG: Mahanadi Graben; 85°ER: 85°E Ridge

Figure 3. Modeled maximum horizontal stress magnitudes and directions for the Wharton Basin area for the late Oligocene (33 Ma) (a), Early Miocene (20 Ma) (b) and present (c). Plotting conventions as in Fig. 1. Outlines of major seamount chains are shown as thin light grey lines, fracture zones from Matthews et al. (2011) as thick black lines and continental crust (Müller et al., 2008a) is grey-shaded. Bold dark-grey lines outline extinct mid-ocean ridges. Strike-slip earthquakes are plotted as filled black circles and earthquakes with thrust faulting and normal faulting mechanisms as filled red circles and blue circles, respectively. Solid stars represent the locations of

intraplate strike-slip earthquakes of magnitude 8.6 and 8.2 occurred in the Wharton Basin on 11th April 2012. NER: Ninetyeast Ridge; WHB: Wharton Basin.

Figure 4. Multichannel seismic reflection sections along profiles 3 (a) and 5 (b), modified from Bastia et al. (2010). See Fig. 2c for locations, labelled as P3 (Profile 3) and P5 (Profile 5). Note the distinct basement-involved folding of the sedimentary section above basement steps/faults around the foot of the continental slope on both profiles, with similar fold amplitudes in the deep and shallow part of the section. Main interpreted horizons are top Eocene, top Oligocene and top Miocene (all in green). The pink and blue horizons represent layers younger than Miocene (but whose exact age is not known), but these lines are drawn to show that the basement-involved folding in P3 is traceable to layers younger than Miocene.

Figure 5. Map of the Indian subcontinent and the adjoining regions showing major faults, rifts and other structural and tectonic trends from Biswas (1982), Bhattacharya and Subrahmanyam (1986) and Mitra (1994) (plotted as thin black lines) along with locations of earthquakes and a colour-coded image of Bouguer gravity anomalies (Balmino et al., 2012). Solid black stars represent locations of earthquakes with magnitudes more than 4.5 and open black stars represent locations of earthquakes whose magnitude is unknown but intensity is greater than VI (Gowd et al., 1996). Fault plane solutions are plotted for the earthquakes whose epicentral source parameters are available from Global Centroid Moment Tensor Catalogue ((Dziewonski et al., 1981; Ekström et al., 2012). The red lines represent fold axes inferred to have formed due to neotectonic events of uplift and subsidence caused by buckling of lithosphere (Bendick and Bilham, 1999). The green lines within the Indian subcontinent represents the major permanent rivers. The dashed magenta line

represents the Mulki-Pulikat Lake Axis (MPLA) (Subrahmanya, 1996), which separates northeast flowing rivers from southeast flowing rivers (shown as thick pink lines). Other details are as in Figure 2. PNR: Penner River; PLR: Palar River.

Figure 6. Magnetic anomalies of the Indian subcontinent from Emag2 (Maus et al., 2009), with the same structural and earthquake data overlain as on Fig. 5. The light blue lines within the Indian subcontinent represents the major permanent rivers. Other details are as in Figures 2 and 5.

Figure 7. Colour-coded image of Bouguer gravity anomalies of the southeastern regions of India showing interpreted line drawings of NE-SW striking undulations (yellow lines) in the region assumed to have been caused by the orthogonal regional maximum horizontal stress field that persisted throughout the Neogene.

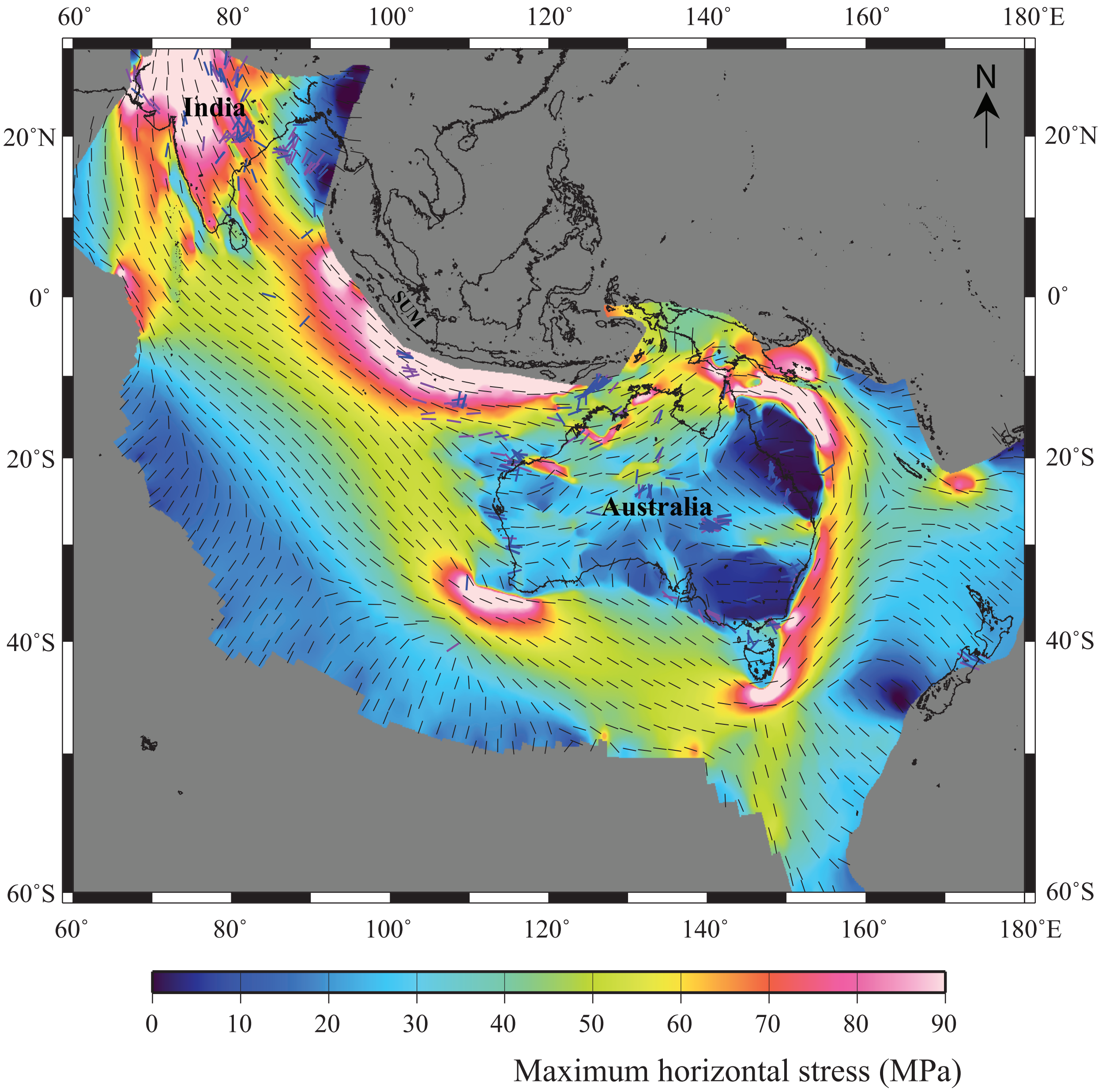
60°
80°
100°
120°
140°
160°
180°E
20°N
0°
20°S
40°S
60°S
N
India
SUM
Australia
0
10
20
30
40
50
60
70
80
90
Maximum horizontal stress (MPa)

804

Figure 1

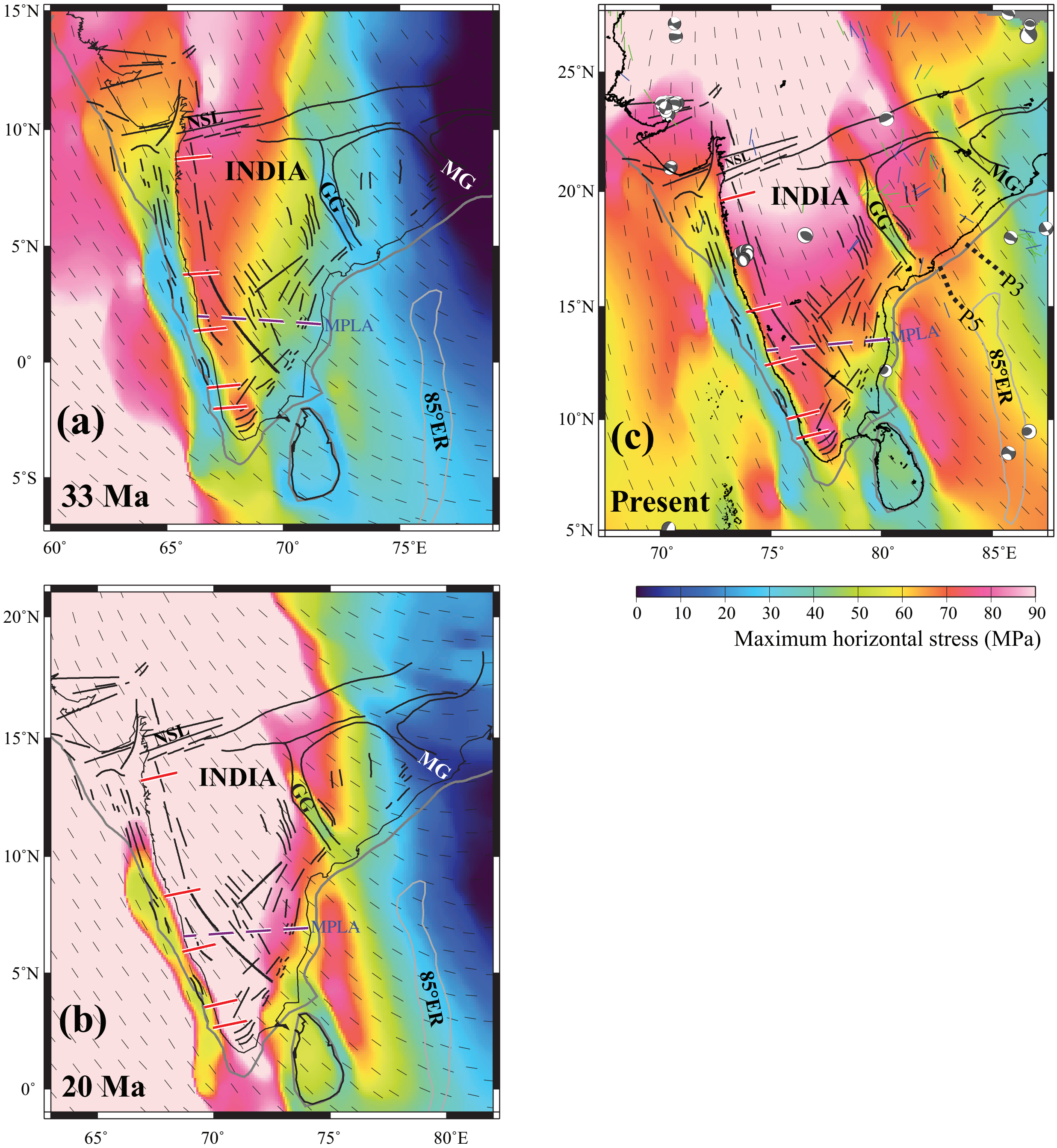
(a)
33 Ma
INDIA
NSL
GG
MG
MPLA
85°ER
15°N
10°N
5°N
0°
5°S
60°
65°
70°
75°E
(b)
20 Ma
INDIA
NSL
GG
MG
MPLA
85°ER
20°N
15°N
10°N
5°N
0°
65°
70°
75°
80°E
(c)
Present
INDIA
NSL
GG
MG
MPLA
P3
P5
85°ER
25°N
20°N
15°N
10°N
5°N
70°
75°
80°
85°E
0
10
20
30
40
50
60
70
80
90
Maximum horizontal stress (MPa)

805

Figure 2

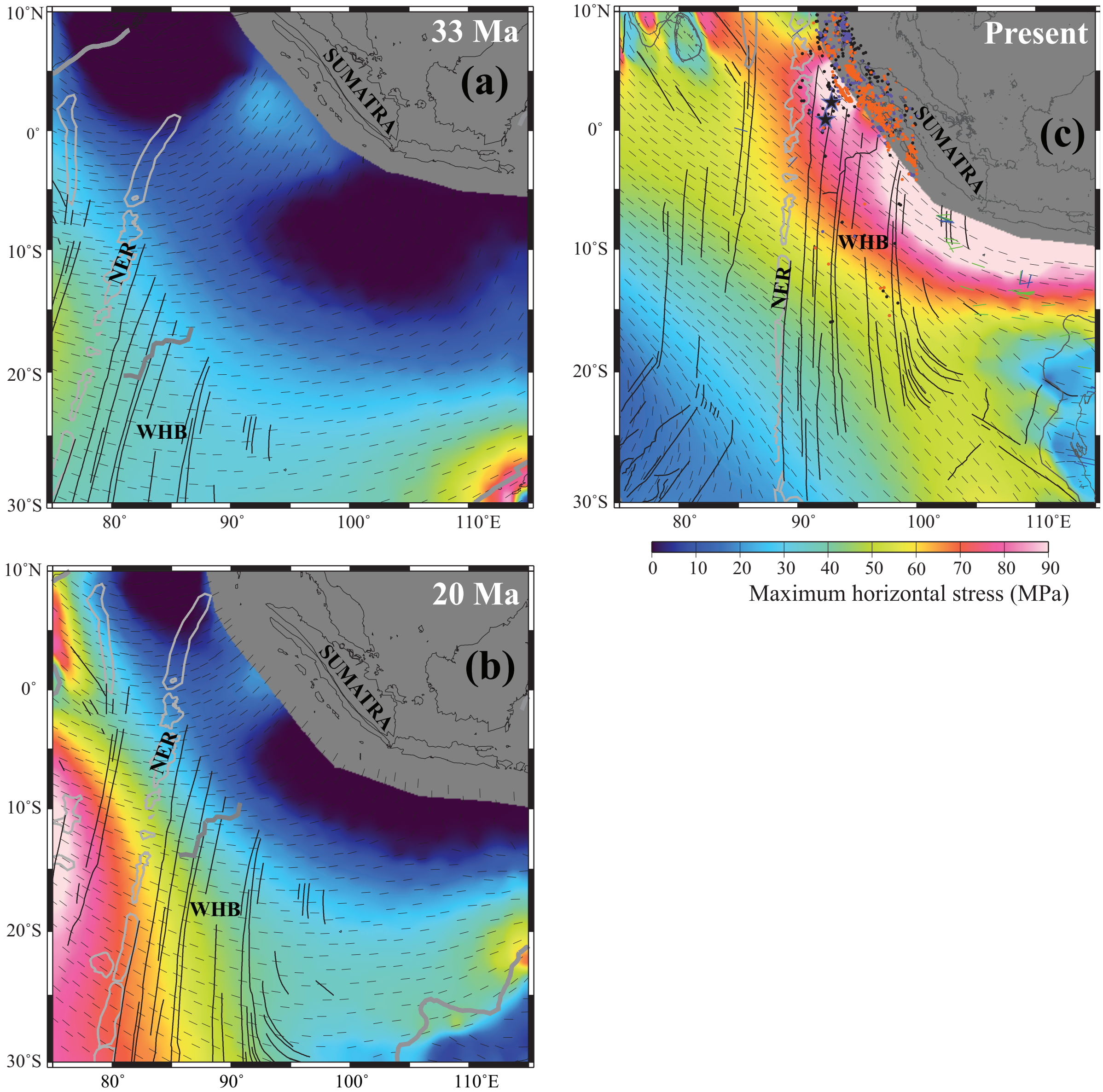
33 Ma
(a)
SUMATRA
NER
WHB
20 Ma
(b)
SUMATRA
NER
WHB
Present
(c)
SUMATRA
NER
WHB
10°N
0°
10°S
20°S
30°S
80°
90°
100°
110°E
0 10 20 30 40 50 60 70 80 90
Maximum horizontal stress (MPa)

Figure 3

806

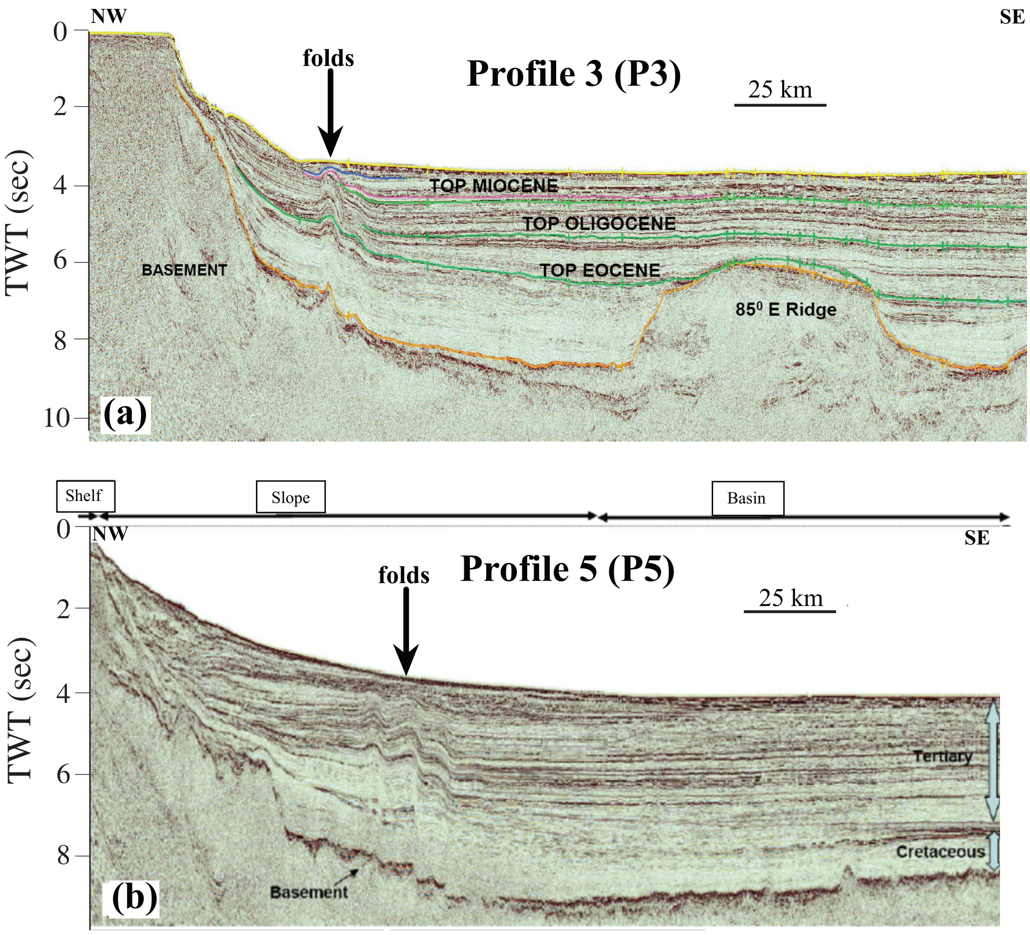
NW
SE
Profile 3 (P3)
folds
25 km
TOP MIOCENE
TOP OLIGOCENE
TOP EOCENE
BASEMENT
85⁰ E Ridge
TWT (sec)
(a)
Shelf
Slope
Basin
NW
SE
Profile 5 (P5)
folds
25 km
Tertiary
Cretaceous
Basement
TWT (sec)
(b)

Figure 4

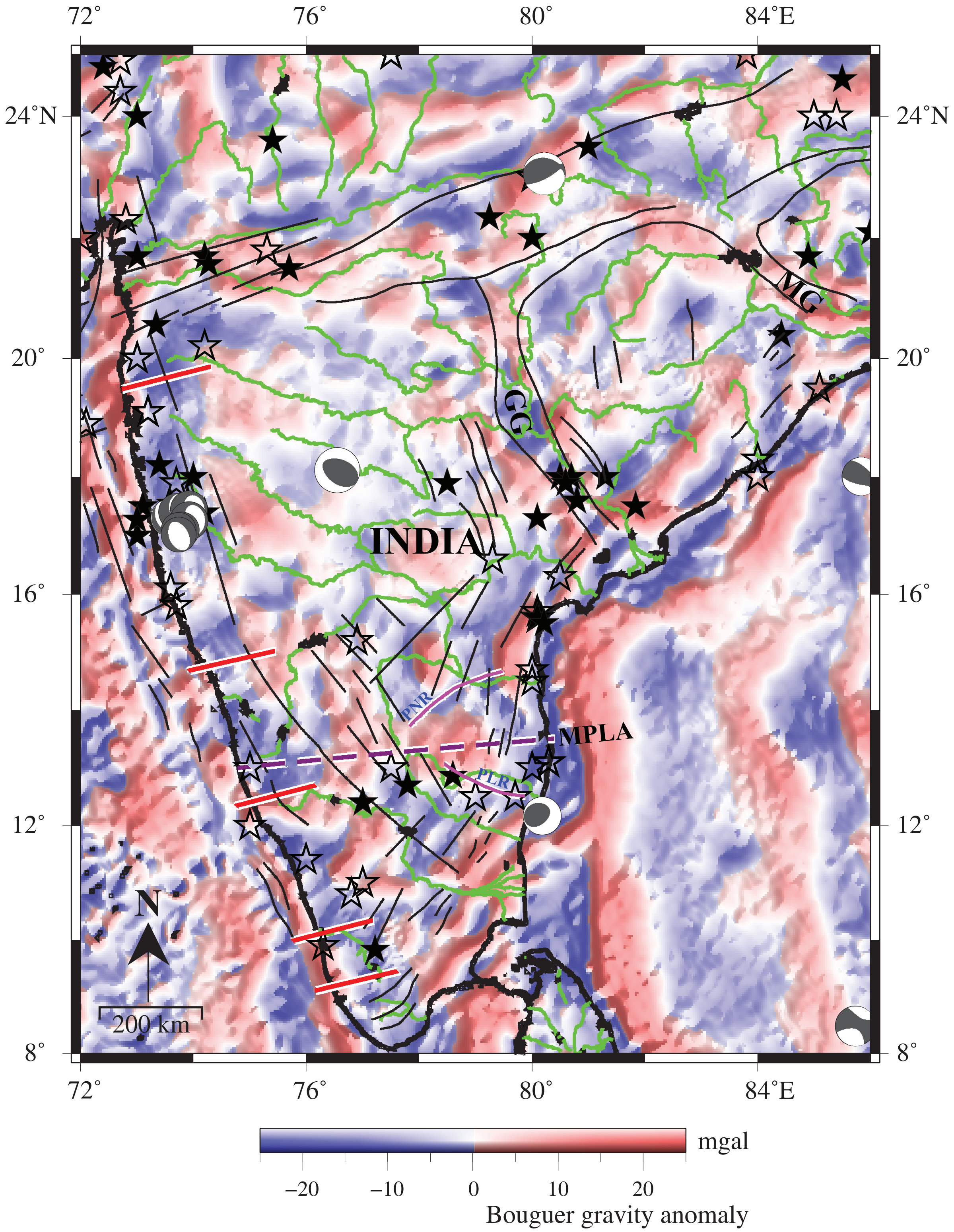
72°
76°
80°
84°E
24°N
20°
16°
12°
8°
INDIA
MG
GG
PNR
MPLA
PLR
N
200 km
mgal
−20
−10
0
10
20
Bouguer gravity anomaly

Figure 5

808

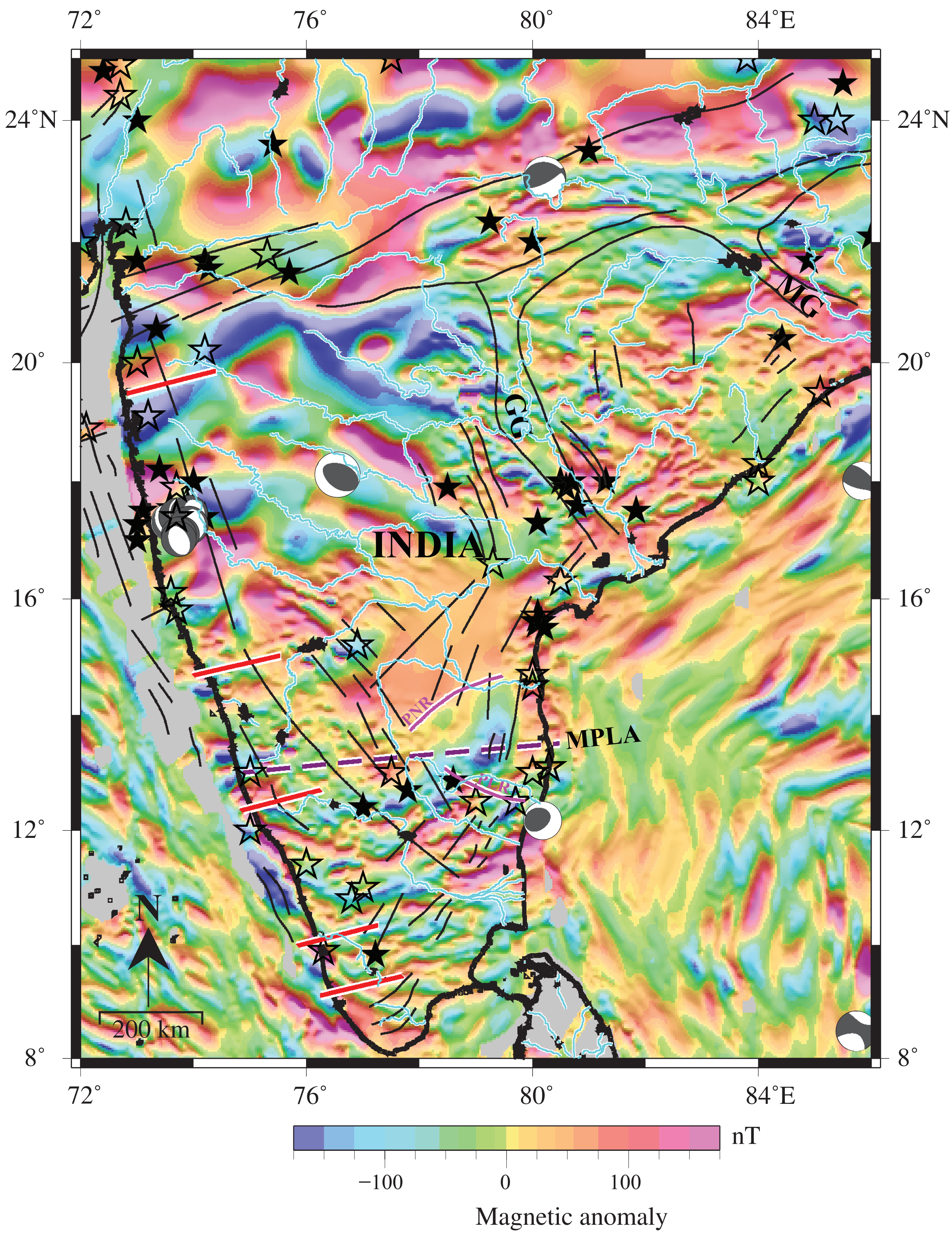

Figure 6

809
810

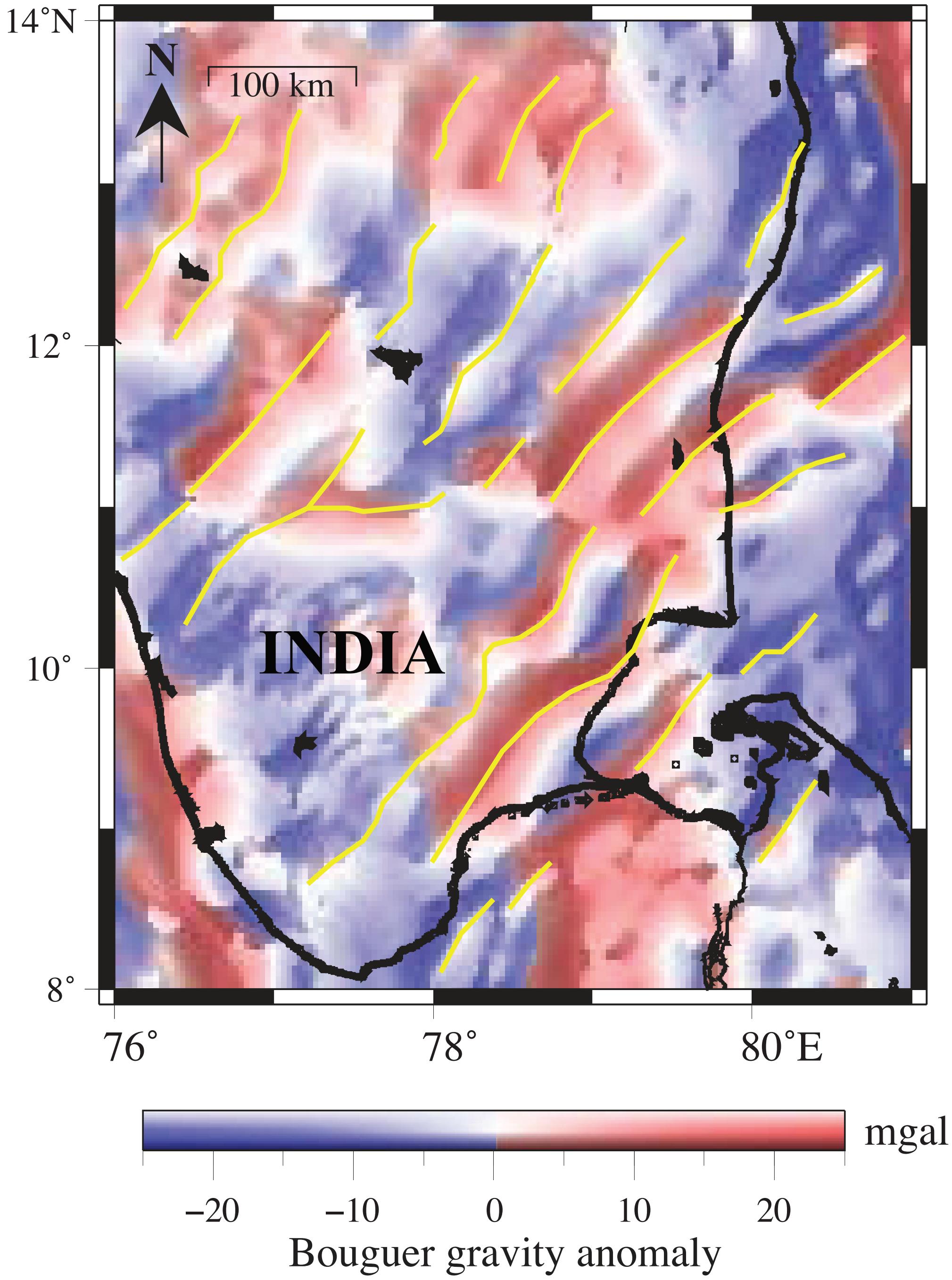
14°N
12°
10°
8°
76°
78°
80°E
N
100 km
INDIA
mgal
−20
−10
0
10
20
Bouguer gravity anomaly

Figure 7

811